Reactions of Silylene with Unreactive Molecules. I: Carbon Dioxide; Gas-Phase Kinetic and Theoretical Studies

Rosa Becerra

Instituto de Quimica-Fisica 'Rocasolano', C.S.I.C., C/Serrano 119, 28006 Madrid, Spain

J. Pat Cannady

Dow Corning Corporation, P.O. Box 995, Mail 128, Midland, Michigan 48686-0995

Robin Walsh*

Department of Chemistry, University of Reading, Whiteknights, P.O. Box 224, Reading, RG6 6AD, U.K.

Received: January 14, 2002; In Final Form: February 21, 2002

Time-resolved studies of the reaction of silylene, SiH_2, with CO_2 have been carried out over the temperature range 298−681 K, using laser flash photolysis to generate and monitor SiH_2. Between 339 and 681 K the reaction obeys second-order kinetics and the derived rate constants gave the following Arrhenius parameters: $\log(A/\mathrm{cm^3\ molecule^{-1}\ s^{-1}}) = -11.89 \pm 0.13$, $E_a = +16.36 \pm 1.23$ kJ mol^{-1}, where the uncertainties are single standard deviations. The reaction shows no overall pressure dependence. This reaction is unusual for SiH_2 in being extremely slow and having a positive activation energy. Ab-initio calculations at the G2 level suggest a mechanism occurring via the intermediacy of siloxiranone (formed via addition of SiH_2 to one of the C═O double bonds) leading to overall formation of $H_2SiO + CO$, consistent with kinetic findings. Direct abstraction of an O atom appears to be ruled out, as are other potential pathways. The mechanism resembles that of $CH_2(^1A_1) + CO_2$.

Introduction

Silylene, SiH_2, is known to react rapidly and efficiently with many chemical species.[1,2] Examples of its reactions include Si−H bond insertions, C═C and C≡C π-bond additions, and reactions with lone pair donors.[3] Many of these reactions occur at close to the collision rate.[1,2] We have recently found that the reactions of SiH_2 with $(CH_3)_2CO$[4] and CH_3CHO[5] are also rapid and thereby shown that silylene addition to the C═O π-bond also conforms to this pattern. Indeed the reaction of SiH_2 with CO itself also fits this behavior at pressures sufficiently high to stabilize the silaketene product, H_2SiCO, although at normal experimental pressures the reaction is quite slow.[6] We therefore decided to investigate the reaction of $SiH_2 + CO_2$, to see whether the affinity of SiH_2 for the carbonyl bond extends even to the highly stable carbon dioxide molecule. We were encouraged in this by the fact that methylene, CH_2 (in its excited $^1A_1$ state, the analogue of ground-state SiH_2) is known to react chemically with CO_2, albeit with a relatively slow rate constant of ca. 1.1×10^{-11} cm^3 molecule^{-1} s^{-1}.[7]

There has been no previous study of this reaction, and so we have undertaken the first gas-phase investigation. We have also carried out quantum chemical calculations, to try to elucidate potential products and reaction pathways. Given both the environmental and the industrial importance of carbon dioxide it is always worth investigating new reactions for it. A preliminary account of this work has been reported.[8]

Experimental Section

Equipment, Chemicals, and Method. The apparatus and equipment for these studies have been described in detail previously.[9,10] Only essential and brief details are therefore included here. SiH_2 was produced by the 193 nm flash photolysis of phenylsilane ($PhSiH_3$) using a Coherent Compex 100 exciplex laser. Photolysis pulses were fired into a variable temperature quartz reaction vessel with demountable windows, at right angles to its main axis. SiH_2 concentrations were monitored in real time by means of a Coherent 699-21 single-mode dye laser pumped by an Innova 90-5 argon ion laser and operating with Rhodamine 6G. The monitoring laser beam was multipassed between 32 and 48 times along the vessel axis, through the reaction zone, to give an effective path length of up to 1.8 m. A portion of the monitoring beam was split off before entering the vessel for reference purposes. The monitoring laser was tuned to 17259.50 cm^{-1}, corresponding to a known strong vibration−rotation transition[9,11] in the SiH_2 $A(^1B_1) \leftarrow X(^1A_1)$ absorption band. Light signals were measured by a dual photodiode/differential amplifier combination and signal decays were stored in a transient recorder (Datalab DL910) interfaced to a BBC microcomputer. This was used to average the decays of up to 10 photolysis laser shots (at a repetition rate of 1 or 2 Hz). The averaged decay traces were processed by fitting the data to an exponential form using a nonlinear least squares package. This analysis provided the values for first-order rate coefficients, k_{obs}, for removal of SiH_2 in the presence of known partial pressures of substrate gas.

Gas mixtures for photolysis were made up, containing between 3.0 and 10.0 mTorr of $PhSiH_3$, and 0−500 Torr of CO_2. In a few experiments total pressures were increased by addition of inert diluent (SF_6). Pressures were measured by capacitance manometers (MKS, Baratroin).

All gases used in this work were thoroughly degassed prior to use. $PhSiH_3$ (99.9%) was obtained from Ventron-Alfa

* Author to whom correspondence should be addressed.

10.1021/jp020091h CCC: $22.00
Published on Web 04/18/2002

(Petrarch). Carbon dioxide, CO_2, (99.999%) was obtained from British Oxygen. Sulfur hexafluoride, SF_6, (no GC-detectable impurities) was from Cambrian Gases.

Ab-Initio Calculations. The electronic structure calculations were performed with the Gaussian 94 software package.[12] All structures were determined by energy minimization at the MP2 = Full/6-31G(d) level. Transition state structures were characterized as first-order saddle points by calculation of the Hessian matrix. Stable structures, corresponding to energy minima, were identified by possessing no negative eigenvalues of the Hessian, while transition states were identified by having one and only one negative eigenvalue. The standard Gaussian-2 (G2) compound method[13] was employed to determine final energies for all structures, both for energy minima and transition states. The identities of the transition state structures were verified by calculation of Intrinsic Reaction Coordinates[14] (IRC) at the MP2 = Full/6-31G(d) level. Reaction barriers were calculated as differences in G2 enthalpies at 298.15 K.

Results

Kinetics. Preliminary experiments quickly established that at ambient temperatures SiH_2 reacts very slowly, if at all, with CO_2. Only at a pressure of 500 Torr was there some sign of reaction. This means that the purity requirement of these experiments is very demanding. Since SiH_2 reacts with many species at or close to the collision rate, small quantities of reactive impurities can give misleading results. Fortunately, the supplied source of CO_2 was very pure. Nevertheless even at impurity levels of only 1 in 10^5, contributions to rates at pressures of 500 Torr may not be negligible. Fortunately reaction rates *increase* with temperature and so the pressures of CO_2 required decrease. Moreover, for most fast reacting species, reaction rates *decrease* with temperature,[1,2] and so impurity problems at higher temperatures will be less serious. Other preliminary checks showed that, for a given reaction mixture, k_{obs} values were not dependent on the exciplex laser energy (50−80 mJ/pulse, routine variation) or number of photolysis shots (up to 10 shots). The constancy of k_{obs} (5 shot averages) showed no effective depletion of reactants. The sensitivity of detection of SiH_2 was very high but decreased with increasing temperature and pressure. Therefore slightly higher quantities of $PhSiH_3$ precursor were required under the latter conditions. For the purposes of rate constant measurement at a given temperature $PhSiH_3$ pressures were kept fixed.

The lowest temperature at which a significant and systematic set of results could be obtained was 339 K. A set of runs was carried out in which the dependence of k_{obs} on CO_2 pressure was investigated (six different pressures up to 500 Torr). Similar sets of runs were carried out at four other temperatures of 398, 473, 583, and 681 K. The results of these experiments are shown in Figure 1, which demonstrates the linear dependence of k_{obs} with $[CO_2]$ expected for second-order kinetics. The second-order rate constants, obtained by least-squares fitting to these plots are collected in Table 1. The error limits are single standard deviations. The lack of curvature in the second-order plots indicates that there is no overall pressure dependence of these rate constants. This was confirmed in a few runs by addition of SF_6 to the reaction mixtures, which resulted in no change of k_{obs} for a given CO_2 pressure.

The data in Table 1 show clearly that the second-order rate constants increase with temperature. An Arrhenius plot of these data is shown in Figure 2. The plot shows curvature, particularly at the lower temperatures. This may be due to a chemical effect (e.g., change of mechanism) but in view of the possibility of impurities affecting the lower rate constants, we prefer to fit the Arrhenius equation to the upper four temperatures only. This yields

$$\log(k/\mathrm{cm^3\ molecule^{-1}\ s^{-1}}) = (-11.89 \pm 0.13) - (16.36 \pm 1.23\ \mathrm{kJ\ mol^{-1}})/RT \ln 10$$

If only the *three* highest temperatures are considered, the Arrhenius parameters increase in value to $\log(A/\mathrm{cm^3\ molecule^{-1}\ s^{-1}}) = -11.69$, $E_a = 18.8$ kJ mol^{-1}. To assist with the mechanistic interpretation of these results we have carried out ab-initio calculations, described in the following section.

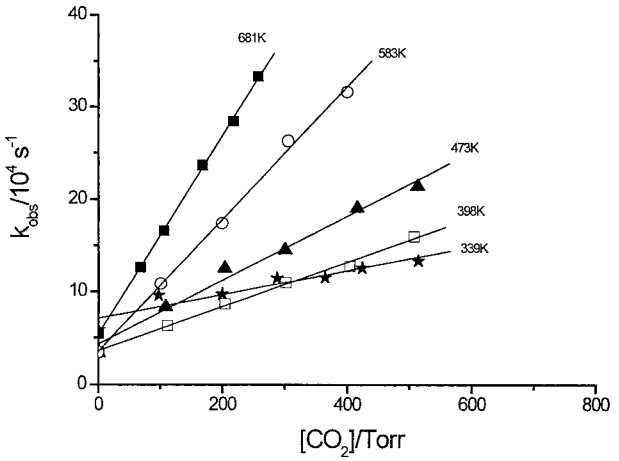

Figure 1. Second-order plots for reaction of SiH_2 with CO_2: (★) 339 K, (□) 398 K, (▲) 473 K, (○) 583 K, (■) 681 K.

TABLE 1: Experimental Second-Order Rate Constants for $SiH_2 + CO_2$ at Several Temperatures

T/K	k/cm^3 molecule^{-1} s^{-1}
298	$(4.2 \pm 0.8) \times 10^{-15}$ [a]
339	$(5.24 \pm 0.55) \times 10^{-15}$
398	$(9.93 \pm 0.25) \times 10^{-15}$
473	$(1.76 \pm 0.07) \times 10^{-14}$
583	$(4.33 \pm 0.10) \times 10^{-14}$
681	$(7.59 \pm 0.07) \times 10^{-14}$

[a] Single point determination.

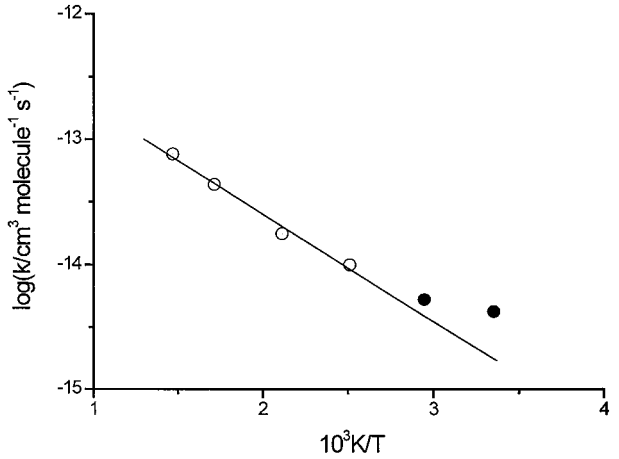

Figure 2. Arrhenius plot of second-order rate constants for $SiH_2 + CO_2$: filled circles not used in least-squares fitting.

Ab-Initio Calculations. Possible species on the CH_2SiO_2 surface were investigated in some detail at the G2 level of theory. Considerable complexity has been found. Apart from the reactant species, $SiH_2 + CO_2$, two plausible final product pairs have been identified, viz, $SiH_2O + CO$ and $CH_2O + SiO$.

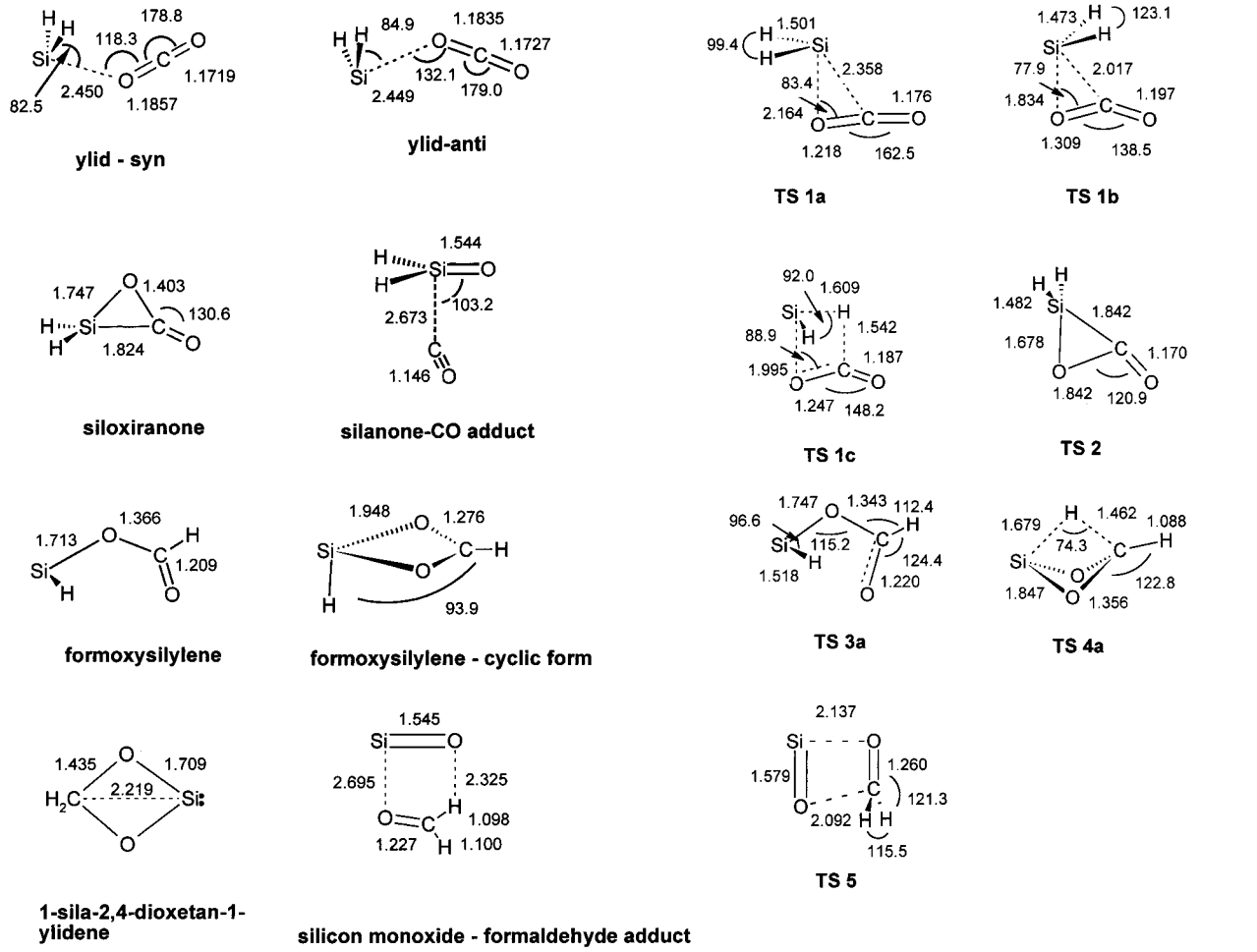

Figure 3. Ab-initio MP2 = Full/6-31G(d) calculated geometries of (a) local minimum structures, and (b) transition states on the CH_2SiO_2 energy surface. Selected distances are given in Å and angles in degrees.

Each product pair is reached via a series of intermediates and transition states.

Pathway (A), leading to $SiH_2O + CO$, traverses three energy minima and two transition states. The minima correspond to the silacarbondioxyl ylid (initial complex of SiH_2 and CO_2; anti form), siloxiranone (α-sila-lactone), and a silanone−carbon monoxide complex. The transition states linking these species are labeled TS1a and TS2. The notable features of this pathway are (i) the initial formation of a fairly weakly bound ylid (weaker than that formed by SiH_2 with other carbonyl species[4,5]), (ii) the slightly positive energy of TS1a (unlike the analogous TS1a linking the ylid and cyclized species for addition to other carbonyl species[4,5] which lie below the reactant energy threshold), and (iii) the very low barrier to rearrangement of siloxiranone.

Pathway (B), leading to $CH_2O + SiO$, traverses five energy minima and four transition states. The minima correspond to the initial ylid (now in the *syn*-form, but again very weakly bound), formoxysilylene (open form), formoxysilylene (cyclic, internally complexed form), 1-sila-2,4-dioxetan-1-ylidene, and a formaldehyde−silicon monoxide complex. The transition states linking these species are labeled TS1c, TS3a, TS4a, and TS5. This pathway is notable for (i) the two lowest energy species on the whole surface, viz., the internally bonded formoxysilylene and the cyclic methylenedioxysilylene, and (ii) the slightly positive energies of TS1c (again unlike the analogous TS1c linking the $H_2Si\cdots OCHCH_3$ adduct with 3-methylsiloxirane which lies below the reactant threshold energy in the SiH_2 + MeCHO reaction system[5]) and TS4a.

TABLE 2: Ab-Initio (G2) Enthalpies for CH_2SiO_2 Species of Interest in the Reaction of Silylene with Carbon Dioxide

molecular species	energy/ hartree	relative energy/ kJ mol^{-1}
$SiH_2 + CO_2$	−478.5216490	0
$H_2Si\cdots CO_2$ ylid-anti	−478.5262930	−12.2
$H_2Si\cdots CO_2$ ylid-syn	−478.5274610	−15.3
TS1a	−478.5172107	+11.7
TS1b	−478.5008445	+54.6
siloxiranone	−478.5495860	−73.3
TS2	−478.5432771	−56.8
$H_2SiO\cdots CO$ complex	−478.5549580	−87.4
$H_2SiO + CO$	−478.5498240	−74.0
TS1c	−478.5130326	+22.6
formoxysilylene	−478.5519850	−79.6
TS3a	−478.5514950	−78.4
formoxysilylene-cyclic	−478.5648870	−113.5
TS4a	−478.5124291	+24.2
1-sila-2,4-dioxetan-1-ylidene	−478.5901230	−179.8
TS5	−478.5366104	−39.3
$H_2CO\cdots SiO$ complex	−478.5587140	−97.3
$H_2CO + SiO$	−478.5466210	−65.6

The structures of all species are shown in Figures 3a and 3b and their enthalpy values are listed in Table 2, as well as being represented on the potential energy (enthalpy) surface in Figure 4. In addition to these potential pathways, some further, high energy, species (and transition states) have also been identified, which are unlikely to be involved in the reaction itself. These species are described in the Appendix; their structures are shown in Figure 5 and energies in Table 4. It should be noted that we

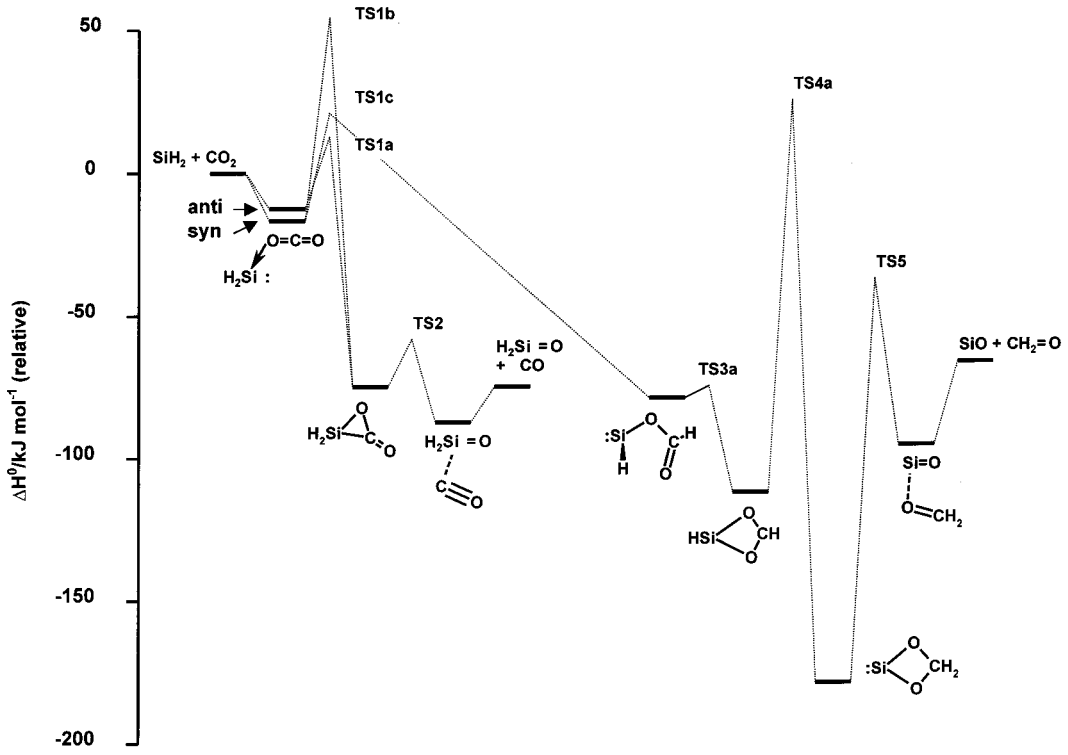

Figure 4. Potential energy (enthalpy) surface for the reaction of $SiH_2 + CO_2$. All enthalpies calculated at the ab-initio G2 level.

TABLE 3: Comparison of Arrhenius Parameters[a] for Additions Reactions of Silylene to Carbonyl and Related Species

reactants	log A^{∞} [b]	E_a/kJ mol^{-1}	k^{∞}(298 K)[a]	ref
$SiH_2 + CO_2$	-11.89 ± 0.13	$+16.4 \pm 1.2$	$<4.2 \times 10^{-15}$	this work
$SiH_2 + CO$	-9.99[c]	-3.0[c]	3.5×10^{-10} [c]	6
$SiH_2 + CH_3CHO$	-10.10 ± 0.06	-3.9 ± 0.5	3.9×10^{-10}	5
$SiH_2 + (CH_3)_2CO$	-10.17 ± 0.04	-4.5 ± 0.3	4.2×10^{-10}	4
$SiH_2 + N_2O$	-12.09 ± 0.04	-2.0 ± 0.3	1.8×10^{-12}	16

[a] High-pressure limiting values. [b] Units: cm^3 molecule^{-1} s^{-1}. [c] Values obtained from expt. data via RRKM assisted extrapolation.

can find no low energy direct O-atom abstraction pathway leading from $SiH_2 + CO_2$ to $H_2SiO + CO$. The search for direct abstraction of the O-atom by SiH_2 from CO_2 gave indications of two possible pathways. One involved a high energy biradical structure some 142 kJ mol^{-1} in energy above the reactants (at the G2 level). However we were unable to identify a transition state structure leading from either the syn- or anti-ylid species to this biradical. The other pathway gave a transition state structure 92 kJ mol^{-1} above the reactants energy (QCISD/6-31G(d) value). IRC calculations showed that this structure was indeed connected to the $H_2SiO\cdots CO$ complex on the product side. However, on the reactant side the IRC calculation ended at a different biradical structure from that described above. We were unable to locate an earlier transition state structure connecting this second biradical to either ylid species by single coordinate variation.The difficulties of more complex IRC calculations led us to abandon this search. However, the high energies of the species on these pathways ensure that, despite the lack of full connectivity, they cannot compete with the lower energy closed-shell pathways (A) and (B).

Discussion

Kinetics, Ab-Initio Calculations, and Mechanism. The results reported here represent the first investigations of the reaction of SiH_2 with carbon dioxide. The data fit reasonably well a linear Arrhenius plot at higher temperatures. If this Arrhenius line represents the true rate constant for $SiH_2 + CO_2$ at 298 K, it corresponds to a value of 1.7×10^{-15} cm^3 molecule^{-1} s^{-1}. The difference between this and the measured value in Table 1, could be accounted for by an impurity in the CO_2 of 1 part in 10^5, reacting on every collision. Since this corresponds to the stated sample purity, we cannot rule this out and therefore we cannot justify attribution of the curvature in the Arrhenius plot to a real effect. The curvature is evident at 298 and 339 K, but might even be present as high as 398 K. However we prefer to attribute the slight deviation from the Arrhenius line at this temperature to scatter and thus we favor the four-temperature over the three-temperature Arrhenius fit.

The Arrhenius parameters obtained are compared with those of other related reactions of SiH_2 in Table 3. It is evident that the parameters for $SiH_2 + CO_2$ are significantly different from those of the reactions of SiH_2 with the other carbonyl species. For SiH_2, reactions with CO, MeCHO, and Me_2CO all occur at close to the collision rate at 298 K, and all have high *A* factors and small negative activation energies. For $SiH_2 + CO_2$, the rate constant at 298 K is at least 5 orders of magnitude slower, has an *A* factor which is ca. 10^2 below the collision number, and also has a positive activation energy. This is the only reaction of SiH_2 (that we are aware of) with a measurable positive activation energy, although the reactions of SiH_2 with CH_4 and $SiMe_4$, which are too slow to be directly studied, must inevitably have (positive) energy barriers.[15] If anything, there is a slight resemblance of the kinetics of $SiH_2 + CO_2$ to those of $SiH_2 + N_2O$.[16] Although this latter reaction is much faster, the *A* factor is rather similar and the difference lies in the activation energies. The low *A* factor suggests some kind of an entropy bottleneck, but the lack of pressure dependence (equally observed for $SiH_2 + N_2O$) indicates no formation of an addition product requiring third body assisted stabilization.

The reaction of $CH_2(^1A_1) + CO_2$ studied by Koch et al.[7] at ambient temperature, occurs with a rate constant of 3.3×10^{-11}

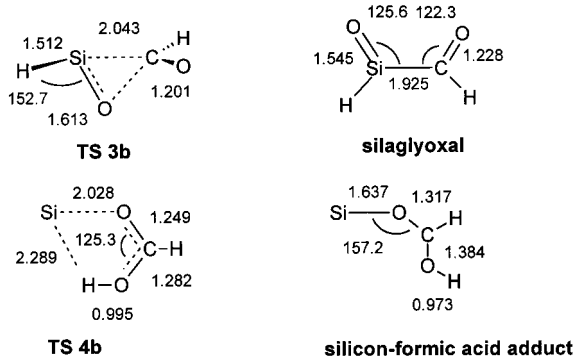

Figure 5. Some further calculated geometries (MP2 = Full/6-31G(d) level) of high energy species on the CH_2SiO_2 energy surface. Selected distances given in Å and angles in degrees.

TABLE 4: Ab-Initio (G2) Enthalpies for Some Further (high energy) Species on the CH_2SiO_2 Energy Hypersurface

molecular species	energy/ hartree	relative energy/ kJ mol^{-1}
$SiH_2 + CO_2$	−478.5216490	0
TS3b	−478.4287951	+243.8
silaglyoxal	−478.5342290	−33.0
TS4b	−478.4550974	+174.7
Si..HCOOH adduct	−478.4572610	+169.1
Si(^{1}D) + HCOOH	−478.4145930	+281.1
Si(^{3}P) + HCOOH	−478.4432340	+205.9

cm^3 molecule^{-1} s^{-1} but only about one-third corresponds to a chemical pathway (the remaining two-thirds comprising collisionally induced intersystem crossing to $CH_2(^3B_1)$). This is considerably faster than the reaction of $SiH_2 + CO_2$ studied here, but Arrhenius parameters for $^1CH_2 + CO_2$ have not been reported. However it has been reported, from matrix isolation studies,[17] that $CH_2O + CO$ are reaction products, probably formed via the intermediacy of α-lactone, viz:

$$^1CH_2 + CO_2 \rightarrow H_2C\begin{matrix}CO\\|\\O\end{matrix} \rightarrow CH_2O + CO$$

Recent ab-initio calculations (G2 level) of the $CH_2 + CO_2$ system by Kovacs and Jackson,[18] show that, on the singlet surface, the lowest energy pathway is indeed that proceeding via the α-lactone. The mechanism via this pathway occurs without activation and, although the α-lactone itself has a significant barrier to decomposition (115 kJ mol^{-1}), the transition state still lies 60 kJ mol^{-1} below the initial energy threshold. The direct O-atom abstraction mechanism has a barrier of 97 kJ mol^{-1}.

For the $SiH_2 + CO_2$ reaction investigated here, the ab-initio calculations point clearly to pathway (A), proceeding via the initial ylid (*anti*-form), through TS1a to siloxiranone and on via TS2 to the $H_2SiO + CO$ products. This pathway is consistent with pressure-independent kinetics, since the cyclic siloxiranone (unlike the siloxiranes[4,5]) is too weakly bound to be pressure stabilized (i.e., by a third body). Furthermore an estimate of the entropy of TS1a of 291 J K^{-1} mol^{-1} (obtained from the ab-initio calculated structure and vibrational wavenumbers) enables us to calculate a value of $\log(A/\text{cm}^3\ \text{molecule}^{-1}\ \text{s}^{-1}) = -11.90$, using the transition state theory expression ($A = e^2(kT/h)\exp(\Delta S^{\ddagger}/R)$).[19] This is in good agreement with the experimental result. Finally the reaction energy barrier via TS1a of 12 kJ mol^{-1} is in very close agreement with the measured activation energy.

The alternative pathway (B) is extremely close in energy terms since TS1c is only 8 kJ mol^{-1} higher in energy than TS1a and within error limits also a possible candidate for the pathway. However, the barrier for the secondary TS4a is 25 kJ mol^{-1} above the reaction threshold and should ensure that, if reaction occurred via TS1c, it would end in the formation of the pressure-dependent, third-body-assisted formation of the stabilized (internally complexed) formoxysilylene. It should also be noted that TS1c is a tighter transition state with a lower *A* factor associated with it. Thus the observed kinetic parameters are not consistent with this pathway.

The direct O-atom abstraction has a significantly positive energy barrier of uncertain magnitude (but at least 92 kJ mol^{-1}), which makes it far too high to be competitive. The Appendix includes details of some other high energy species on the CH_2SiO_2 surface. Overall the $SiH_2 + CO_2$ reaction shows considerable similarity to the $^1CH_2 + CO_2$ reaction, with the main difference being the small positive energy barrier to the formation of the cyclic lactone product in the silicon case. This is probably a reflection of the lesser stability of the sila-α-lactone ring (−71 kJ mol^{-1}) compared with the α-lactone ring (−176 kJ mol^{-1}) arising from two causes, viz., (i) the extra stabilization (DSSE) of SiH_2 relative to CH_2[20] and (ii) increased strain in the ring in the silicon case. The high affinity of silicon for oxygen-containing species (and C═O double bonds) is clearly not enough to overcome these factors.

Acknowledgment. R.B. and R.W. thank Dow-Corning for a grant in support of the experimental work. R.B. also thanks the Spanish DGICYT for support under Projects PB98-0537-C02-01 and BQU2000-1163-C02-01.

Appendix: Further Species on the CH_2SiO_2 Energy Surface

In addition to the likely potential pathways and intermediate species, two higher energy pathways have been identified. Pathway (C) starting from formoxysilylene (open form) involves a 1,2 CHO-migration from O− to Si− via TS3b to yield silaglyoxal. Pathway (D) stating from formoxysilylene (closed form) involves a 1,2 H-migration via TS4b to yield an Si atom···formic acid complex which dissociates with a small extra energy into Si (^{3}P or ^{1}D) + formic acid. These structures and their energies are shown in Figure 5 and Table 4, respectively.

References and Notes

(1) Jasinski, J. M.; Becerra, R.; Walsh, R. *Chem. Rev.* **1995**, *95*, 1203.

(2) Becerra, R.; Walsh, R. Kinetics & mechanisms of silylene reactions: A prototype for gas-phase acid/base chemistry. In *Research in Chemical Kinetics*; Compton, R. G., Hancock, G., Eds.; Elsevier: Amsterdam, 1995; Vol. 3, p 263.

(3) Gaspar, P. P.; West, R. Silylenes. In *The Chemistry of Organic Silicon Compounds*; Rappoport, Z., Apeloig, Y., Eds.; Wiley: Chichester, 1998; Vol. 2, Chapter 43, p 2463.

(4) Becerra, R.; Cannady, J. P.; Walsh, R. *J. Phys. Chem. A* **1999**, *103*, 4457.

(5) Becerra, R.; Cannady, J. P.; Walsh, R. *Phys. Chem. Chem. Phys.* **2001**, *3*, 2343.

(6) Becerra, R.; Cannady, J. P.; Walsh, R. *J. Phys. Chem. A* **2001**, *105*, 1897.

(7) Koch, M.; Temps, F.; Wagener, R.; Wagner, H. G. *Ber. Bunsen-Ges. Phys. Chem.* **1990**, *94*, 645.

(8) Becerra, R.; Cannady, J. P.; Walsh, R. 33rd Organosilicon Symposium, Saginaw, Mich., April 6−8, 2000; paper B-11.

(9) Baggott, J. E.; Frey, H. M.; King, K. D.; Lightfoot, P. D.; Walsh, R.; Watts, I. M. *J. Phys. Chem.* **1988**, *92*, 4025.

(10) Becerra, R.; Frey, H. M.; Mason, B. P.; Walsh, R.; Gordon, M. S. *J. Chem. Soc., Faraday Trans.* **1995**, *91*, 2723.

(11) Jasinski, J. M.; Chu, J. O. *J. Chem. Phys.* **1988**, *88*, 1678.

(12) Frisch, M. J.; Trucks, G. W.; Schlegel, H. B.; Gill, P. M. W.; Johnson, B. G.; Robb, M. A.; Cheeseman, J. R.; Keith, T.; Petersson, G. A.; Montgomery, J. A.; Raghavachari, K.; Al-Laham, M. A.; Zakrzewski, V. G.; Ortiz, J. V.; Foresman, J. B.; Cioslowski, J.; Stefanov, B. B.; Nanayakkara, A.; Challacombe, M.; Peng, C. Y.; Ayala, P. Y.; Chen, W.; Wong, M. W.; Andres, J. L.; Replogle, E. S.; Gomperts, R.; Martin, R. L.; Fox, D. J.; Binkley, J. S.; Defrees, D. J.; Baker, J.; Stewart, J. P.; Head-Gordon, M.; Gonzales, C.; Pople, J. A. *Gaussian 94*, Revision E.2; Gaussian Inc.: Pittsburgh, 1995.

(13) Curtiss, L. A.; Raghavachari, K.; Trucks, G. W.; Pople, J. A. *J. Chem. Phys.* **1991**, *94*, 7221.

(14) Gonzales, C.; Schlegel, H. B. *J. Chem. Phys.* **1989**, *90*, 2154.

(15) Becerra, R.; Walsh, R. *Int. J. Chem. Kinet.* **1999**, *31*, 393.

(16) Becerra, R.; Frey, H. M.; Mason, B. P.; Walsh, R. *Chem. Phys. Lett.* **1991**, *185*, 415.

(17) Milligan, D. E.; Jacox, M. E. *J. Chem. Phys.* **1962**, *36*, 2911.

(18) Kovacs, D.; Jackson, J. E. *J. Phys. Chem. A* **2001**, *105*, 7579.

(19) Benson, S. W. *Thermochemical Kinetics*, 2nd ed.; Wiley: New York, 1976.

(20) Becerra, R.; Walsh, R. Thermochemistry. In *The Chemistry of Organic Silicon Compounds*; Rappoport, Z., Apeloig, Y., Eds.; Wiley: Chichester, 1998; Vol. 2, Chapter 4, p 153.